XXII INTERNATIONAL CONFERENCE ON
"MATERIAL HANDLING, CONSTRUCTIONS AND LOGISTICS"

4th - 6th October, 2017

MHCL 2017

Edited by
Nenad Zrnić, Srđan Bošnjak and Georg Kartnig

UNIVERSITY OF BELGRADE
Faculty of Mechanical Engineering
VIENNA UNIVERSITY OF TECHNOLOGY (TU WIEN)
Institute for Engineering Design and Logistics Engineering

BELGRADE, SERBIA, 2017

UNIVERSITY OF BELGRADE
Faculty of Mechanical Engineering

TECHNISCHE UNIVERSITÄT WIEN
Vienna University of Technology

XXII INTERNATIONAL CONFERENCE ON
"MATERIAL HANDLING, CONSTRUCTIONS AND LOGISTICS"

4th – 6th October, 2017

MHCL 2017

Edited by

Nenad Zrnić, Srđan Bošnjak and Georg Kartnig

UNIVERSITY OF BELGRADE
Faculty of Mechanical Engineering

VIENNA UNIVERSITY OF TECHNOLOGY (TU WIEN)
Institute for Engineering Design and Logistics Engineering

BELGRADE, SERBIA, 2017

INTERNATIONAL SCIENTIFIC COMMITTEE

Co-Chairmen:

Prof. Dr. Nenad Zrnić, University of Belgrade, Serbia
Prof. Dr. Srđan Bošnjak, University of Belgrade, Serbia
Prof. Dr. Georg Kartnig, Vienna University of Technology, Austria

Members of Scientific Committee:

Prof. Dr. Bidanda Bopaya, University of Pittsburgh, USA
Prof. Dr. Bogdevicius Marijonas, Vilnius Gediminas Technical University, Lithuania
Prof. Dr. Bošnjak Srđan, University of Belgrade, Serbia
Prof. Dr. Ceccarelli Marco, University of Cassino, Italy
Prof. Dr. Chondros Thomas, University of Patras, Greece
Prof. Dr. Clausen Uwe, TU Dortmund, Fraunhofer Institute for Material Flow and Logistic, Germany
Prof. Dr. Ćuprić Nenad, University of Belgrade, Serbia
Prof. Dr. Czmochowski Jerzy, Wroclaw University of Science and Technology, Poland
Prof. Dr. Dentsoras Argiris, University of Patras, Greece
Prof. Dr. Dragović Branislav, University of Montenegro, Kotor, Montenegro
Prof. Dr. Đukić Goran, University of Zagreb, Zagreb, Croatia
Prof. Dr. Edl Milan, University of West Bohemia, Plzen, Czech Republic
Prof. Dr. Ekren Banu, Yaşar University, Turkey
Prof. Dr. Furmans Kai, Karsruhe Institute of Technology, Germany
Prof. Dr. Gašić Milomir, University of Kragujevac, Kraljevo, Serbia
Prof. Dr. Gašić Vlada, University of Belgrade, Serbia
Prof. Dr. Georgiev Martin, Technical University Sofia, Bulgaria
Prof. Dr. Georgijević Milosav, University of Novi Sad, Serbia
Prof. Dr. Gerhard Detlef, Vienna University of Technology, Austria
Prof. Dr. Guenthner Wilibald, TU Munich, Germany
Prof. Dr. Hrabovsky Leopold, Technical University of Ostrava, Czech Republic
Prof. Dr. Illes Bela, University of Miskolc, Hungary
Prof. Dr. Jančevski Janko, Ss. Cyril and Methodius University Skopje, Republic of Macedonia
Prof. Dr. Jerman Boris, University of Ljubljana, Slovenia
Prof. Dr. Jodin Dirk†, Graz University of Technology, Austria
Prof. Dr. Jovanović Miomir, University of Niš, Serbia
Prof. Dr. Kartnig Georg, Vienna University of Technology, Austria
Prof. Dr. Katterfeld Andre, Otto-von-Guericke-Universitat Magdeburg, Germany
Prof. Dr. Kessler Franz, Montan University of Leoben, Austria
Prof. Dr. Kosanić Nenad, University of Belgrade, Serbia
Prof. Dr. Lerher Tone, University of Maribor, Slovenia
Prof. Dr. Markusik Sylwester, Silesian University of Technology, Gliwice, Poland
Prof. Dr. Mitrović Radivoje, University of Belgrade, Serbia
Prof. Dr. Ognjanović Milosav, University of Belgrade, Serbia
Prof. Dr. Oguamanam C.D. Donatus, Ryerson University Toronto, Ontario, Canada
Prof. Dr. Overmeyer Ludger, Leibniz University Hannover, Germany
Prof. Dr. Park Nam Kyu, Tongmyong Univ. of Information Technology, Busan, South Korea
Prof. Dr. Popović Vladimir, University of Belgrade, Serbia
Prof. Dr. Potrč Iztok, University of Maribor, Slovenia
Prof. Dr. Rakin Marko, University of Belgrade, Serbia
Prof. Dr. Rosi Bojan, University of Maribor, Slovenia
Prof. Dr. Rogić Miroslav, University of Banja Luka, Republic of Srpska, Bosnia and Herzegovina
Prof. Dr. Rusinski Eugeniusz, Wroclaw University of Science and Technology, Poland
Prof. Dr. Sari Zaki, University of Tlemcen, Algeria
Prof. Dr. Savković Mile, University of Kragujevac, Serbia
Prof. Dr. Sawodny Oliver, University of Stuttgart, Germany
Prof. Dr. Schmidt Thorsten, Dresden University of Technology, Germany
Prof. Dr. Schott Dingena, Delft University of Technology, The Netherlands
Prof. Dr. Sihn Wilfried, Vienna University of Technology, Fraunhofer Austria, Austria
Prof. Dr. Singhose William, Georgia Institute of Technology, Atlanta, USA
Prof. Dr. Solazzi Luigi, University of Brescia, Italy
Prof. Dr. ten Hompel Michael, TU Dortmund, Fraunhofer Institute for Material Flow and Logistic, Germany
Prof. Dr. Vidović Milorad, University of Belgrade, Serbia

Prof. Dr. Vladić Jovan, University of Novi Sad, Serbia
Prof. Dr. Wehking Karl-Heinz, University of Stuttgart, Germany
Prof. Dr. Weigand Michael, Vienna University of Technology, Austria
Prof. Dr. Wimmer Wolfgang, Vienna University of Technology, Austria
Prof. Dr. Wypych Peter, University of Wollongong, Australia
Prof. Dr. Zrnić Nenad, University of Belgrade, Serbia

President of Honorary Scientific Committee and Conference Founder:

Prof. Dr. Đorđe Zrnić, University of Belgrade, Serbia

Members of Honorary Scientific Committee:

Prof. Dr. Babin Nikola, University of Novi Sad, Serbia
Prof. Dr. Hoffmann Klaus, Vienna University of Technology, Austria
Prof. Dr. Mijajlović Radić, University of Niš, Serbia
Prof. Dr. Oser Joerg, Graz University of Technology, Austria
Prof. Dr. Ostrić Davor, University of Belgrade, Serbia
Prof. Dr. Petković Zoran, University of Belgrade, Serbia
Prof. Dr. Severin Dietrich, Technical University of Berlin, Germany
Prof. Dr. Zrnić Đorđe, University of Belgrade, Serbia

ORGANIZING COMMITEE

Presidents of the Organizing Committee:

Prof. Dr. Nenad Zrnić, University of Belgrade, Serbia
Prof. Dr. Georg Kartnig, Vienna University of Technology, Austria

Vice President of the Organizing Committee:

Prof. Dr. Branislav Dragović, University of Montenegro, Montenegro

Members of Organizing Committee:

Gašić Vlada, University of Belgrade, Serbia
Gnjatović Nebojša, University of Belgrade, Serbia
Milojević Goran, University of Belgrade, Serbia
Đorđević Miloš, University of Belgrade, Serbia
Milenović Ivan, University of Belgrade, Serbia
Stefanović Aleksandar, University of Belgrade, Serbia

Reviewers:

Prof. Dr. Bošnjak Srđan, Serbia
Prof. Dr. Dragović Branislav, Montenegro
Prof. Dr. Jerman Boris, Slovenia
Prof. Dr. Kartnig Georg, Austria
Prof. Dr. Lerher Tone, Slovenia
Prof. Dr. Papadimitriou Stratos, Greece
Prof. Dr. Zrnić Nenad, Serbia

Publisher:

University of Belgrade, Faculty of Mechanical Engineering

Printout:

„Planeta Print" d.o.o., Belgrade, Serbia

CIRCULATION: **100 copies**

ISBN 978-86-7083-949-6

Georg Havlicek
Project Assistant
Vienna University of Technology
Faculty of Mechanical and Industrial Engineering
Institute for Engineering Design and Logistics Engineering

Stefan Krenn
Scientist
Excellence Centre of Tribology
AC²T research GmbH

Georg Kartnig
Professor
Vienna University of Technology
Faculty of Mechanical and Industrial Engineering
Institute for Engineering Design and Logistics Engineering

Determination of the longitudinal creep of a driven crane wheel on a crowned rail

The longitudinal creep on a crane wheel has considerable effects, both for the design and the control of the drive technology of a modern crane. The creep occurring during operation is, however, widely unknown. This article presents a calculation model for longitudinal creep of a driven crane wheel, which can be used for a fast analytical determination. Based on the contact area between the crane wheel and the rail an equivalent line contact is calculated instead of the complex real point contact situation. The approach was validated at the institute's wheel-rail test rig.

Keywords: *Longitudinal creep, crane wheel, rail-wheel-contact, analytic method, running-in characteristic*

1. INTRODUCTION

Currently applicable standards for crane design (DIN EN 13001 and sub-standards [1]) consider only rail geometries with flat heads at the contact between crane wheel and rail. Nowadays, crowned rails are used almost exclusively. As a result of the wear-specific run-in behavior, a change in the rail head profile occurs with increasing operating time (overrun cycles). This also results in a change of the initially ideal elliptical contact surface to an approximate line contact geometry, but not over the entire width of the railhead.

For this reason, a research project was launched in 2014 at the Department of Transport, Handling and Conveying Systems (KLFT) in cooperation with Hans Künz GmbH, which aims at transferring existing approaches of the static and structural design for the flat rail head to the general case of a cambered rail. The effects of the modified rail geometry on relevant system parameters, e.g. contact pressure, rolling friction, skewing forces, longitudinal creep, adhesion and wear of wheel and rail are to be investigated. Furthermore, the characteristics of the run-in behavior of the rail head due to plastic deformation are considered in the context of the project.

In 2016 the Excellence Center of Tribology (AC²T) was included in the project to achieve a better understanding of the tribological aspects within the contact surface.

In this publication, the longitudinal (tangential) slip between a driven or braked crane wheel and a cambered rail is to be described in more detail.

For various reasons it is necessary to know the occurring slip:

- The maximum transferable braking and driving force depends on the slip ratio (i.e. traction).
- The utilization of the coefficient of static friction is associated with higher slip ratios and higher wear.
- Different wheel loads on the individual wheels result in different slip ratios. Production tolerances on the wheel diameters also result in different circumferential forces on the wheels and thus deviating slip values. The crane clamps or distorts itself according to different wheel speeds.

However, actual slip values at the crane wheel during operation are widely unknown. Therefore an application-oriented and quick-to-calculate analytical approach for the longitudinal slip of current cranes is desirable.

When considering slippage a fundamental distinction between micro-slip (creep) and macro-slip (sliding) needs to be done. In the case of creep, the contact surface is subdivided into a stick zone with the same speed and a slip zone with a relative speed between the contact partners. The coefficient of static friction is the limiting factor for the tangential force that can be transmitted. If the slippage becomes larger, the stick zone disappears and the slip zone extends over the entire contact surface. From this point on there is pure sliding (macro-slip), and the coefficient of sliding friction is decisive (see Figure 1). On a driven or braked wheel, macro-slip corresponds to wheelspin, which in principle is to be avoided in crane construction. All slip curves considered in this work concern the micro-slip region.

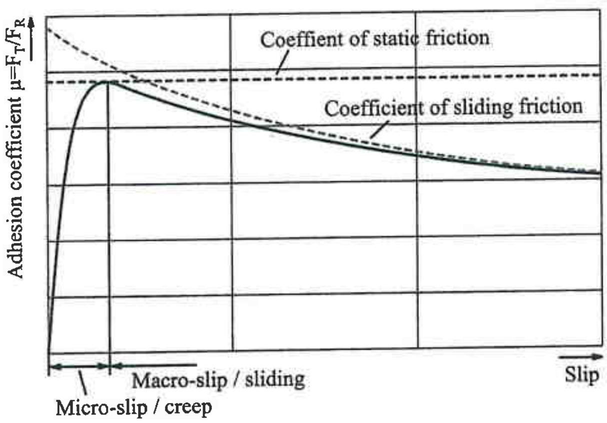

Figure 1. Traction-creep-relation (qualitative)

Correspondence to: Dipl.-Ing. Georg Havlicek
Technische Universität Wien,
Getreidemarkt 9/301-7, 1060 Vienna, Austria
E-mail: georg.havlicek@tuwien.ac.at

2. EXISTING CALCULATION APPROACHES

The following calculation approaches are only described with respect to the tangential slip ratio. Axial slip and spin (rotation around the vertical axis) are not considered in this work, as far as the calculation methods are concerned. Furthermore, a contact geometry between a crane wheel and a crane rail according to DIN 536 has been given [2].

The tangential slip is generally defined as a related velocity difference between the circumferential speed of the wheel and the absolute velocity.

$$\xi_T = \frac{R\,\omega - V}{\max(R\,\omega, V)} \tag{1}$$

2.1 Calculation approach for line contact according to Carter

For the slip-bearing contact of a cylinder with a plane, relationships for longitudinal creep were derived by F.W. Carter [3] as early as 1926. These were again completely elaborated by G. Heinrich and K. Desoyer [4] and extended to incorporate lateral slip effects.

The following relationship for the longitudinal creep is obtained as a function of the contact force F_R, the circumferential force at the wheel F_T, the wheel radius R, the contact width in the contact b_K, the coefficient of static friction μ_0 and material constants G and v. [4]

$$\xi_T = \sqrt{\frac{4}{\pi}\frac{1-v}{G}\frac{F_R}{R\,b_K}}\;\mu_0\left(1-\sqrt{1-\frac{F_T}{\mu_0\,F_R}}\right) \tag{2}$$

Figure 2 shows the contact area as well as the shear stress distribution in the contact surface between the rolling cylinder and the plane under radial load and transmission of a torque.

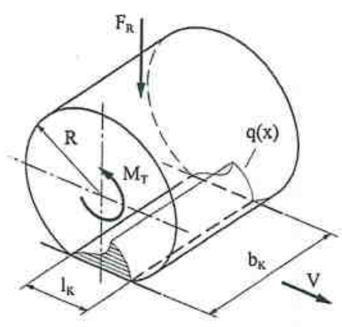

Figure 2. Contact between cylinder and plane

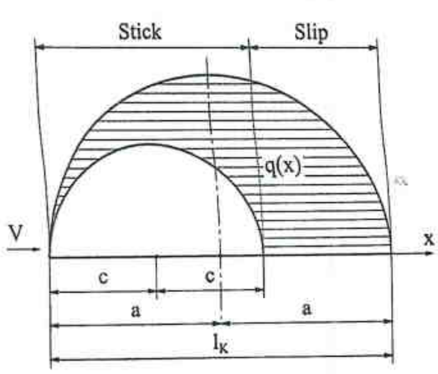

Figure 3. Distribution of shear stress and division in slip and stick zone in contact

Along the contact length l_K, the division into the slip and stick zone as well as the shear stress distribution as shown in Figure 3 are obtained.

The last term of Equation (2) corresponds to the proportion of the stick zone over the entire contact length and is a determining parameter for the creep.

$$a^* = \frac{c}{a} = \sqrt{1-\frac{F_T}{\mu_0\,F_R}} \tag{3}$$

The relationship between the contact length and the contact width for a line contact according to Hertz is included in Equation (2).

$$\frac{l_K}{2} = \sqrt{\frac{8}{\pi}\frac{(1-v)^2}{E}\frac{F_R\,R}{b_K}} \tag{4}$$

Thus, the formula can be rewritten to use the length instead of the width of the contact surface. Along this length the division into stick and slip zone is also determined.

$$\xi_T = \frac{l_K}{2\,R}\,\mu_0\left(1-\sqrt{1-\frac{F_T}{\mu_0\,F_R}}\right) \tag{5}$$

The correctness of the approach was confirmed by J.J. Kalker amongst others using numerical methods [5].

For the contact between a crane wheel and a flat rail head, Equations (2) or (5) can be used right away. Certain deviations to the real contact situation between the wheel and the rail are to be expected since the approach does not take any edge effects at the boundary surfaces of the cylinder into account.

2.2 Calculation approaches for point contact

Approaches for calculating the slip conditions at point contact, as occurs with a cambered rail head, are not trivially solved. The transmitted tangential force is not constant over the width of the contact surface (here the long semi-axis of the contact ellipse). The distribution of the shear stress and the separation in the slip and stick zone of the contact surface is shown in Figure 4.

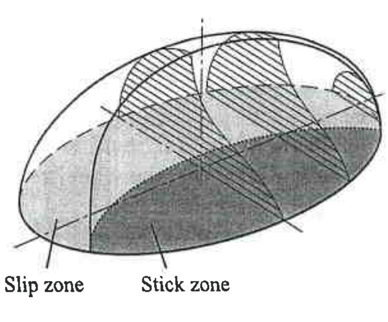

Figure 4. Shear stress distribution at point contact (qualitative)

Strip theory by Haines and Ollerton

The strip theory is a pure analytical calculation method, in which the elliptical contact surface is divided into thin strips parallel to the rolling direction and then integrated. Each individual strip is treated as a line but any influence of the strips on each other is ... The approach of B.J. Haines and E. Ollerton ... tangential creep was elaborated by J.J. Kalker ... developed further in order to be able to take ... creep and a small proportion of spin into ... [6, 7, 8]. Figure 5 shows the discretization of the ... surface and the shear stress distribution in the ...

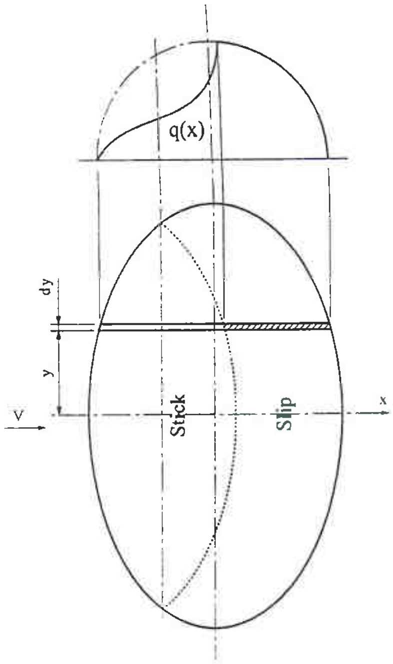

...ure 5. Strip theory according to Haines and Ollerton

The relationship between tangential force and creep ...defined by:

$$F_T = \mu_0 F_R \left\{ \tfrac{3}{2}\zeta\cos^{-1}(\zeta) + \left[1-\left(1+\tfrac{1}{2}\zeta^2\right)\sqrt{1-\zeta^2}\right]\right\} \quad (6)$$

...with the factor ζ as a function of the slip ξ_T and the ...rtzian pressure p_0 in the contact.

$$\zeta = \xi_T \frac{E}{2\,\mu_0\,(1+\nu)\,p_0} \quad (7)$$

The results of this calculation method correspond ...ry well with experimental results and numerical ...thods for slender contact areas (half-axis ratio ...≈ 0.2). If, however, the contact surfaces deviate ...verely from this shape, the errors become large due to ...e lack of influence of the strips on each other [7].

The theory was not pursued further after the ...velopment of the simplified theory of Kalker in favor ...the more exact numerical calculation.

...merical methods according to Kalker

Calculation models of the exact and simplified theory ...veloped by Kalker can only be solved numerically. ...ey are implemented in the contact models of the ...ograms CONTACT (exact) and FASTSIM ...mplified). Both models divide the contact area into ...ctangular parts, which must be balanced in relation to ...e stress state over the entire contact surface. The exact Kalker theory provides accurate results. At pure tangential stress on the contact the simplified theory deviates by up to 5% [9].

For more information on the numerical methods according to Kalker, see [5] and [10].

Linear method according to Kalker

This theory uses the numerically determined Kalker coefficients for the relation between slip and tangential stress. These are defined in tabular form as a function of the half-axis lengths of the contact ellipse and the Poisson ratio. Interpolations are necessary for intermediate values. The linear theory is applicable only for very small slip values since the existence of a slip zone is neglected in this approach. It represents the slope of the linear branch of the creep curve from the origin. Larger slip values caused by the influence of the increasing slip zone are not reproduced correctly. The deviation of the linear theory from the real creep curve is shown qualitatively in Figure 6.

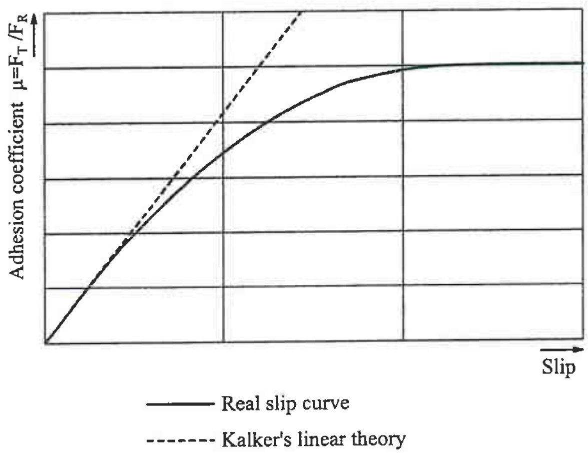

Figure 6. Discrepancy linear theory and real creep curve

According to Kalker's linear theory the dependence of the tangential force on the longitudinal creep is defined via the following relation:

$$F_T = G\,a\,b\,C_{11}\,\xi_T \quad (8)$$

For the purely tangential contact problems, only the Kalker coefficient C_{11} is required. (For values see [5].)

3. CALCULATION APPROACH FOR THE ACTUAL CONTACT GEOMETRY

The actual contact geometry between the crane wheel and the rail does not correspond to an ideal point contact after a short operating time of the crane system. Due to plastic deformation, the curvature of the rail head changes until the stresses inside the rail no longer exceed the yield point.

Imprints recorded using pressure measuring films already show run-in behavior on a new crane during the commissioning phase, which leads to a leveling of the rail head. Due to the limited measuring range of the Fujifilm Prescale films, the occuring contact pressures cannot be evaluated, but they provide very good information about the shape of the contact surface. Figure 7 shows the measuring film on the crane rail after loading by the crane wheel. Figure 8 shows the resulting imprint on the film. In addition, the calculated contact ellipse of an ideal point contact is superimposed. Since the crane has was moved across the film, the exact contour of the contact area is not visible, but the contact width is significantly greater than the result according to Hertz's theory.

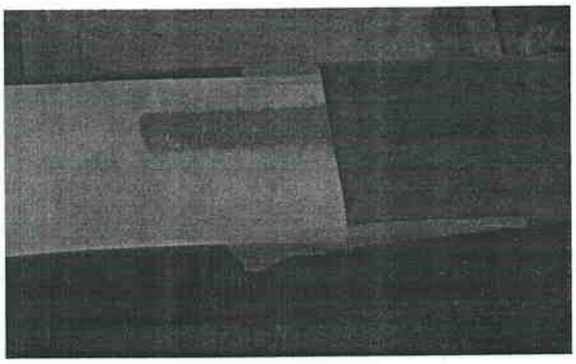

Figure 7. Fujifilm pressure measurement film on crane rail

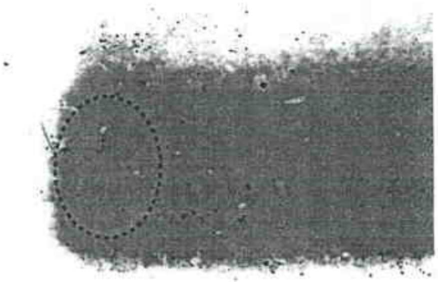

Figure 8. Imprint of the contact surface and theoretical contact ellipse

The contact width stabilizes after a certain time, so that even in the case of cranes that have been in operation for years, the contact surface does not extend over the full width of the rail. As an example of this a photograph of a crane rail after approximately seven years of operation is shown in Figure 9.

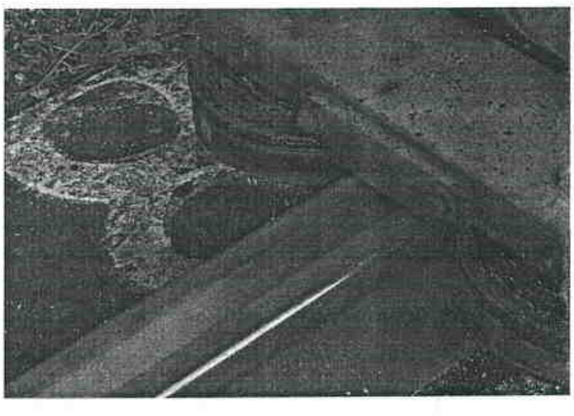

Figure 9. Run-in crane rail

Similar running-in behavior also takes place at the test rig at the Institute for Engineering Design and Logistics Engineering at the Vienna University of Technology described in more detail in Section 4. After approximately twenty operating hours with maximum wheel load the camber of the rail-wheel is flattened to a permanent geometry. Figure 10, taken at a load of 50 kN, compares a recorded imprint to the theoretical contact ellipse according to Hertz.

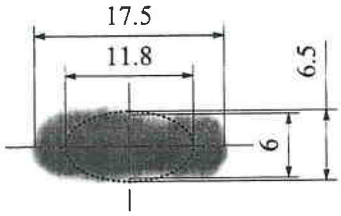

Figure 10. Run-in contact area (dimensions in mm)

For the calculation of the creep ratios for such real contact surfaces, the following approach uses the method for line contact according to Carter as well as Heinrich and Desoyer. This is adapted in such a way that a fictitious linear contact is calculated in which the average tangential stress in the contact surface coincides with the actual contact situation.

For pure tangential slippage the length in the direction of movement (l_{real}) has been identified as a determinant measure for the size of the contact surface. If the width of the fictitious contact surface is calculated according to the Hertzian theory for line contact as a function of the contact force and this contact length, the same surface areas as in the case of the real contact surfaces are obtained. Figure 11 shows two imprints, on the right a run-in rail, on the left in a new condition. The rectangle drawn corresponds to the fictitious contact surface used for slip calculation.

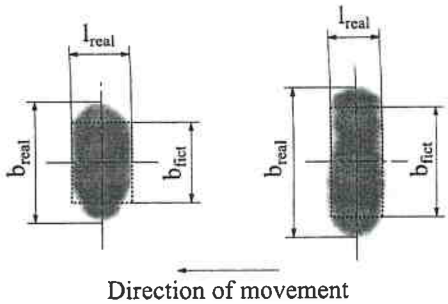

Figure 11. Dimensions of the contact areas (left: new, right: run-in)

This correspondence of the surface areas was only checked for the field of application and the geometries of crane wheels and rails. In the case of strongly divergent forms of the contact surfaces, the validity of this relationship would have to first be verified.

The essential procedure for determining the slip of a wheel according to this method is as follows:

When considering a new crane, or assuming that the wheel loads are sufficiently low to prevent plastic deformation, the required contact length l_{real} can be determined by the Hertzian theory. The half-axis length of the contact ellipse in the direction of motion can be used as a good approximation for the contact length.

If the slip on a run-in crane system is to be calculated, a determination of the real contact area is necessary. How and to which geometry a crane rail runs in is part of the investigations at the Vienna University of Technology, but the contact surface cannot yet be estimated after plastic deformation. A measurement by means of pressure measurement films represents a simple and favorable solution. The crane wheel to be evaluated is lifted by means of hydraulics and put back on the rail r the film has been placed. After two minutes of osure, the film is removed again and the impression be measured directly. Figure 12 shows an imprint on ujifilm Prescale film.

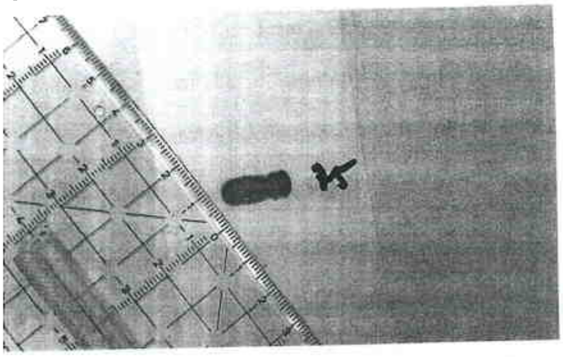

jure 12. Fujifilm Prescale pressure measurement film th imprint

After determining the contact length l_{real}, the creep rve can be computed without difficulty with Equation) from Section 0:

$$\xi_T = \frac{l_{real}}{2\,R}\,\mu_0 \left(1 - \sqrt{1 - \frac{F_T}{\mu_0\,F_R}}\right) \qquad (9)$$

Additionally required factors for the calculation are e radius of the wheel R, the coefficient of static friction :tween wheel and rail μ_0 (according to DIN 13001-3-3 the range of 0.1 to 0.3), the wheel load F_R, and the ngential force F_T to be transmitted. A requirement for ie validity of the approach are identical elastic :operties of the wheel and rail materials (modulus of asticity and Poisson's ratio).

The division of the contact surface into the slip and ick zone, which is decisive for the slip, is determined n the basis of the contact length used, and is assumed to e constant for the entire contact width.

For a common configuration of a portal crane in the ew state, the creep curves shown in Figure 13 result rom this approach.

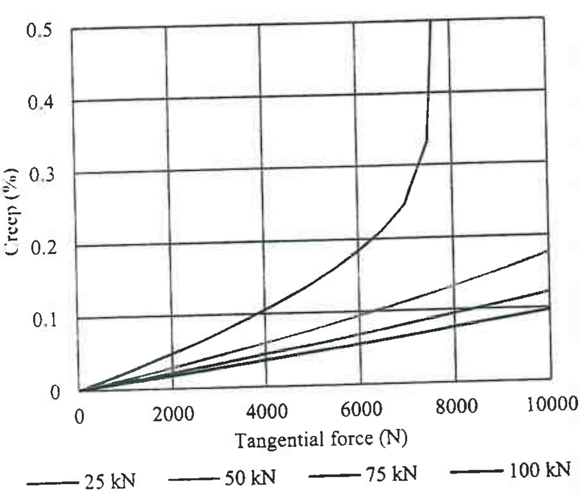

Figure 13. Creep over tangential force at various wheel loads

Contact details:

Radius of the crane wheel	$R = 315$ mm
Radius of the railhead	$R_S = 500$ mm
Coefficient of static friction	$\mu_0 = 0.3$
Radial forces (wheel loads)	$F_R = 25, 50, 75$ and 100 kN
Tangential forces	$F_T = 0$ to $10{,}000$ N

The dimensions of the real contact surface in this case are calculated using the Hertzian theory for two generally curved bodies (see [11]).

The adhesion limit is reached with the assumed coefficient of static friction of $\mu_0 = 0.3$ and a wheel load of 25 kN at $F_T = 7500$ N. The creep values go to infinity with a tangential force $F_T > \mu_0 F_R$. The real elliptical and the fictitious rectangular contact areas were calculated for comparison and plotted in Table 1.

Table 1. Dimensions of the contact areas

Radial force	Hertzian contact lenght	Hertzian area elliptic	Area fictitious rectangle	Deviation
25 kN	7 mm	52 mm²	52.1 mm²	+0.4%
50 kN	8.8 mm	82.5 mm²	82.8 mm²	+0.4%
75 kN	10.1 mm	108 mm²	108.5 mm²	+0.4%
100 kN	11.1 mm	130.9 mm²	131.4mm²	+0.4%

The results of this simplified analytical calculation approach are to be validated in the following section with measurements on a wheel-rail test stand.

4. DETERMINATION OF TANGENTIAL CREEP AT THE TEST STAND.

In order to examine the running behavior of crane wheels on a cambered rail, a test stand was developed and built in cooperation with Künz. Test stands of this type were already used in the 1970s and 80s to research the flat rail head. The wheel-rail test rig at the KLFT (Figure 14) consists of a rail bent to a circular ring (rail-wheel) and a crane wheel. Both wheels can be independently driven and braked. The contact force of the wheel can be specified via hydraulic cylinders. On both drive units there are incremental encoders to detect the exact position of the wheels. The rail-wheel has a diameter of 2000 mm and a head shape corresponding to a rail of the form A55 according to DIN 536, while the crane wheel has a diameter of 400 mm.

In the case of slip measurements, the crane wheel is driven without power limitation, and the rail-wheel brakes with a defined torque. After precise determination of the diameter ratio, the rotational angle difference between the wheel and the rail is used to calculate the creep values after a defined number of revolutions. Beforehand, the contact area is determined using Fujifilm pressure measuring films for each load step.

The measurements were carried out at various conditions of the rail as well as at various friction values. In order to influence the coefficient of friction between the wheel and the rail, conditioning agents, also in combination with water, were applied to the rail surface. Since a flattening of the rail head radius occurs on the test stand, in the same way as for a real crane rail, measurement runs were carried out in the run-in state first. After completion of the measurements in the run-in,

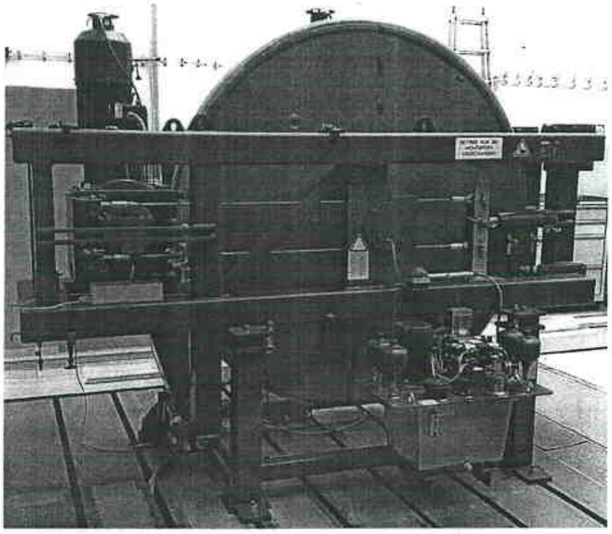

Figure 14. Wheel-rail test stand at KLFT, TU Wien

realistic state, the rail-wheel was re-profiled and the rail geometry corresponding to the new state was restored. In this state a real point contact with an elliptical contact surface can be measured at low radial forces. These measurements were used in order to be able to validate the analytical approach also with this contact geometry.

4.1 Measurements in the run-in state

The measurements were carried out at wheel loads (radial forces) of 25 to 100 kN. At each force, the braking torque was varied between 250 and 1750 Nm, which corresponds to a tangential force in the contact area of 1250 to 8750 N. For all combinations of tangential force and wheel load, at least three valid measuring points were recorded and averaged.

The evaluation of the contact areas shows that the contact width increases only slightly in the run-in state. The radius of curvature has flattened in the center of the head of the rail, so the actual contact ellipse is no longer recognisable. Figure 15 shows the contact surfaces for the radial forces of 25 to 100 kN. The fictitious rectangular contact surfaces of the analytical approach are already drawn.

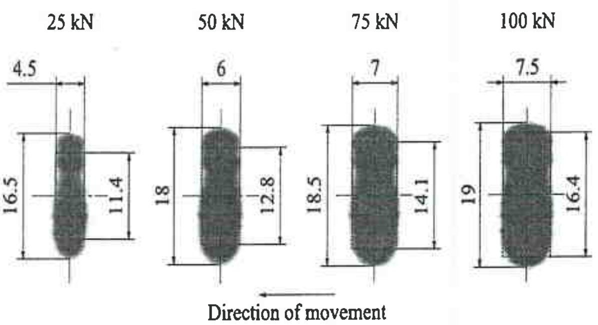

Figure 15. Contact areas on test stand at 25 to 100 kN wheel load (dimensions in mm)

After analyzing the pressure measuring films in the program GODAV the surface areas of the real and fictitious contact surfaces can be compared.

Table 2. Dimensions of the contact areas on the test stand

Radial-force	Real contact lenght	Real contact area	Fictitious contact area	Deviation
25 kN	4.5 mm	52.5 mm²	51.3 mm²	-2.2%
50 kN	6 mm	86 mm²	77 mm²	-10.4%
75 kN	7 mm	108 mm²	99 mm²	-8.3%
100 kN	7.5 mm	127 mm²	123.2 mm²	-3.0%

Figure 16 compares the results of the measurements in the run-in, dry, unconditioned state with the analytical approach. The drawn creep values were averaged from five measurement runs.

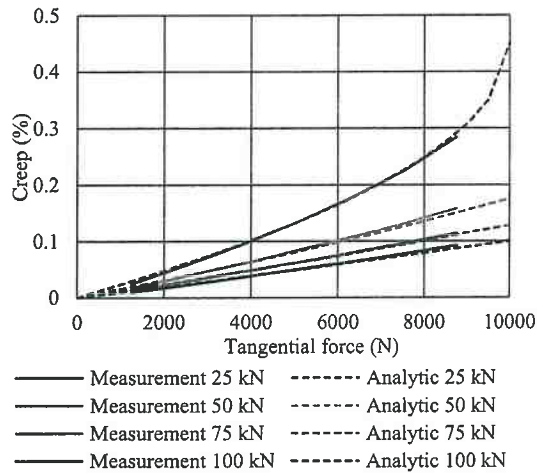

Figure 16. Creep over tangential force, measurement and analytical approach (dry, run-in state)

The slip curves end at the maximum torque that can be applied via the rail wheel drive. The coefficient of static friction between wheel and rail was determined as $\mu_0 \approx 0.4$ in previous measurements. It exhibits very good agreement between measured and analytically calculated creep values.

The dependence of the creep curves on the coefficient of friction between wheel and rail is shown in Figure 17 where the results in the conditioned state are plotted.

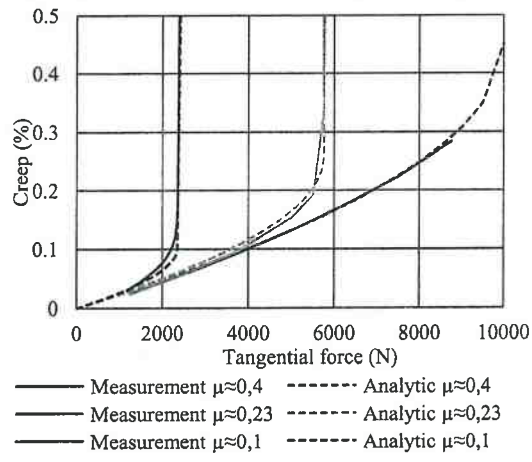

Figure 17. Creep over tangential force, measurement and analytical approach at 25 kN (conditioned, run-in state)

With the aid of solid lubricants, the coefficient of static friction was reduced from $\mu_0 \approx 0.4$ to $\mu_0 \approx 0.23$ and in further measurements to $\mu_0 \approx 0.1$. Again, one can see the very good compliance between analytically calculated and measured slippage.

For a contact force of 25 kN, the measured curves of the creep for the different friction values are drawn. For the two lower friction values, the maximum transmittable force of $F_T = \mu_0 \cdot F_R$ is reached. When the maximum tangential force is approached, the measured slip becomes infinite and can no longer be determined with the available measuring equipment. At this point, the transition from creep to sliding occurs.

4.2 Measurements in new condition

The measurements with actual point contact were carried out only at 25 and 50 kN radial force, since at higher loads the plastic deformation in the rail material leads to the running-in of the geometry. Figure 18 compares the measured curve of the creep with the calculation approach for a dry rail, and in Figure 19 the corresponding contact areas are shown.

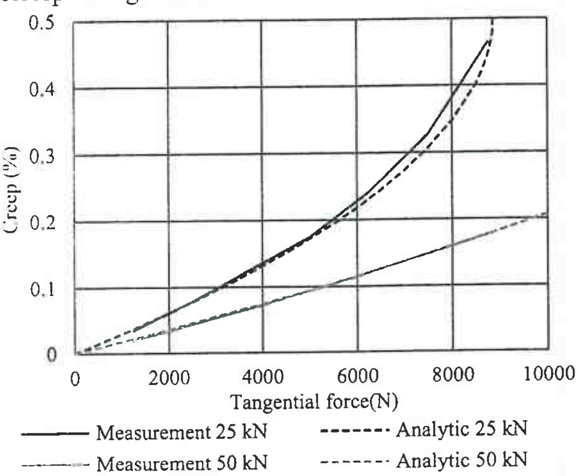

Figure 18. Creep over tangential force, measurement and analytical approach (dry, new condition)

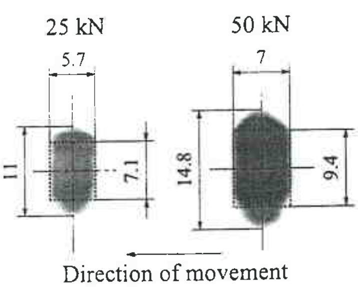

Figure 19. Contact areas on test bench at 25 and 50 kN wheel load in new condition (dimensions in mm)

These measurements prove that the chosen approach also provides good results for point-shaped contact geometries.

5. Summary and Outlook

The approach of Carter for line contact is successfully applied to a point-shaped contact geometry. The assumptions made, using an average tangential stress over the surface, as well as a constant division in stick and slip zone over the entire contact width, do not seem to have any significant effect on the creep. Compared with the measurements at the test rig, very good agreement with the analytical calculation approach is achieved both for various friction values as well as for various contact geometries. In the case of a known contact area, the creep curve can also be determined for a run-in state in a fast manner without long computing times.

In further ongoing studies, the consistency of the slip ratios at the fictitious and the real contact surface is examined more precisely by means of finite element methods. Due to the wider possibilities of variation of the contact geometry in the FEM calculations, the validity limits of the analytical approach can also be determined.

ACKNOWLEDGMENT

Significant parts of this work were funded by the "Austrian COMET-Programme" (Project XTribology, no. 849109) and were developed in collaboration with the "Excellence Centre of Tribology" (AC²T research GmbH).

REFERENCES

[1] DIN EN 13001-3: Krane – Konstruktion allgemein – Parts 3-1 to 3-3.

[2] DIN 536-1: Kranschienen Form A.

[3] Carter, F.W. "On the action of a locomotive driving wheel." *Proceedings of the Royal Society of London A: Mathematical, Physical and Engineering Sciences*. Vol. 112. No. 760. The Royal Society, 1926.

[4] Heinrich, G., and K. Desoyer. "Rollreibung mit axialem Schub." *Ingenieur-Archiv* 36: 48-72, 1967.

[5] Kalker, J.J. *Rolling contact phenomena.* Springer, Vienna, 2000.

[6] Haines, D.J., and E. Ollerton. "Contact stress distributions on elliptical contact surfaces subjected to radial and tangential forces." *Proceedings of the Institution of Mechanical Engineers* 177: 95-114, 1963.

[7] Kalker, J.J. "A Strip Theory for Rolling With Slip and Spin. I.-IV." *Koninklijke Nederlandse Akademie van Wetenschappen-Proceedings Series B-Physical Sciences* 70: 10-62, 1967.

[8] Johnson, K.L. *Contact mechanics*. Cambridge University Press, 1987.

[9] Vollebregt, E.A.H., and P. Wilders. "FAST-SIM2: a second-order accurate frictional rolling contact algorithm." *Computational Mechanics* 47: 105-116, 2011.

[10] Kalker, J.J. *Three-dimensional elastic bodies in rolling contact*. Springer Science & Business Media, 1990.

[11] Timoshenko, S., and J.N. Goodier. *Theory of Elasticity*. McGraw-Hill book Company, Third Edition, 1970.

NOMENCLATURE

a	Half-axis of the contact ellipse in the direction of movement (half the contact length)
a^*	Proportion of the stick zone of the contact length
b_{fict}	Fictitious contact width for creep calculation
b_K	Contact width (width of the contact area)
b_{real}	Real (measured) contact width
c	Half length of the stick zone
C_{ii}	Kalker-Coefficient
E	Modulus of elasticity
F_R	Radial force (wheel load)
F_T	Tangential force (traction force)
G	Shear modulus
l_K	Contact length (length of the contact area)
l_{real}	Real (measured) contact length
M_T	Traction moment
p_0	Hertzian stress
q	Shear stress
R	Radius crane wheel
R_S	Head radius rail
V	Absolute velocity
ζ	Factor for slip calculation
μ	Adhesion coefficient
μ_0	Coefficient of static friction
v	Poisson's ratio